Journal of the European Ceramic Society 20 (2000) 1017–1021

Finite element modelling of the electrical impulse induced fracture of a high voltage varistor

Markus Lengauer*, Domagoj Rubeša, Robert Danzer

Christian-Doppler-Laboratorium at the Department of Structural and Functional Ceramics, University of Leoben, Peter-Tunner-Straße 5, 8700 Leoben, Austria

Received 3 March 1999; received in revised form 24 August 1999; accepted 12 September 1999

Abstract

In testing and in service, varistors are subjected to very short (μs range) high current pulses. Due to the inertia effects that appear on rapid Joule heating dynamic stress waves are generated, which can cause brittle failure. An analytical solution for the one-dimensional case was presented recently by Vojta and Clarke. In this work a full three-dimensional analysis of an axisymmetrical varistor has been performed using Finite Element Simulation. The reflections of the stress waves from the bases and the shell of a varistor and their interference are analyzed. The resulting stress field and its development with time is much more complex than in the 1D case. The aspect ratio of the varistor has been shown to have a strong influence on the amplitude of the mechanical stresses and can be varied to minimize the maximum stress level reached. Damping has been considered but found to be negligible in realistic cases.

Keywords: Failure analysis; Finite element methods; Fracture; Varistors; Electrical pulses

1. Introduction

Varistors are cylindrical electrical resistor components whose resistivity strongly decreases with the applied voltage. They are commonly used to protect electrical devices against voltage pulses. In service they can fail due to puncture failure, pulse induced fracture and long-term degradation of electrical properties.[1] This paper addresses to the pulse induced fracture, which may occur during standardized screening testing of varistors with high current pulses of very short duration (of some μs). This loading situation has recently been discussed in details by Vojta and Clarke.[1] Using an analytical one-dimensional model they analyzed stress waves generated by inertial forces that appear on rapid Joule heating. These stresses strongly depend on the duration of the pulse. In a 1D-model the only design parameter is the length of the varistor. It was concluded that the stress amplitude increases with increasing the length.

In the present paper, the analysis is extended to a full three-dimensional simulation using the finite element method (FEM).[2,3] This makes it possible to consider not only the reflections of stress waves from the bases of the cylinder but also from its shell. After a short description of the numerical model, the time dependent stress fields are analysed with and without damping. The model is then used to optimize the design of the varistor in order to minimize the maximum stress level reached.

2. Model description

The conceptual basis of the model is described in detail in the paper of Vojta and Clarke[1] and the theoretical background can be found e.g. in Ref. 4. During electrical loading of a varistor electrical energy is converted into heat. This Joule effect occurs by electron–phonon interactions and is, therefore, very quick. As a consequence of heating the material tends to expand. If this process is quick, inertial forces can not be neglected. In this paper we concentrate on the problem of a free-standing varistor: at any time its bases and the shell are considered to be traction-free. Compressive stress wave generated by the electrical loading pulse is totally reflected at the surfaces and interacts with the original wave leading to a complicated interference picture.

* Corresponding author at Pankl R&D GmbH, Kaltschmidstrasse 2-6, 8600 Bruck a.d. Mur, Austria

E-mail address: lengauer@pankl.co.at (M. Lengauer).

0955-2219/00/$ - see front matter
PII: S0955-2219(99)00249-6

2.1. Loading

The electric power load shown in Fig. 1a is a standardized impulse used for the testing of varistors. This so called 4″10 impulse reaches 90% of the maximum peak value of power in 4 μs and after 10 μs it falls to 50% of the peak value. Very similar loading has been applied in the work of Vojta and Clarke.[1] It is assumed, that the varistor is uniformly heated by this pulse. Heat transfer from the varistor to the surroundings can be neglected, since the time considered is very short (i.e. in the μs range).

The raise in temperature T at the time t, caused by the Joule heating, is given by

$$T(t) = T_0 + \frac{1}{mc_v}\int_0^t P(\tau)\mathrm{d}\tau, \quad (1)$$

where T_0 is the uniform initial temperature of the varistor (taken to be 25°C) at $t = 0$, m is the mass, c_v is the specific heat capacity at a constant volume, and P is the electric power. The temperature raise corresponding to the electric power load in Fig. 1a is presented in Fig. 1b.

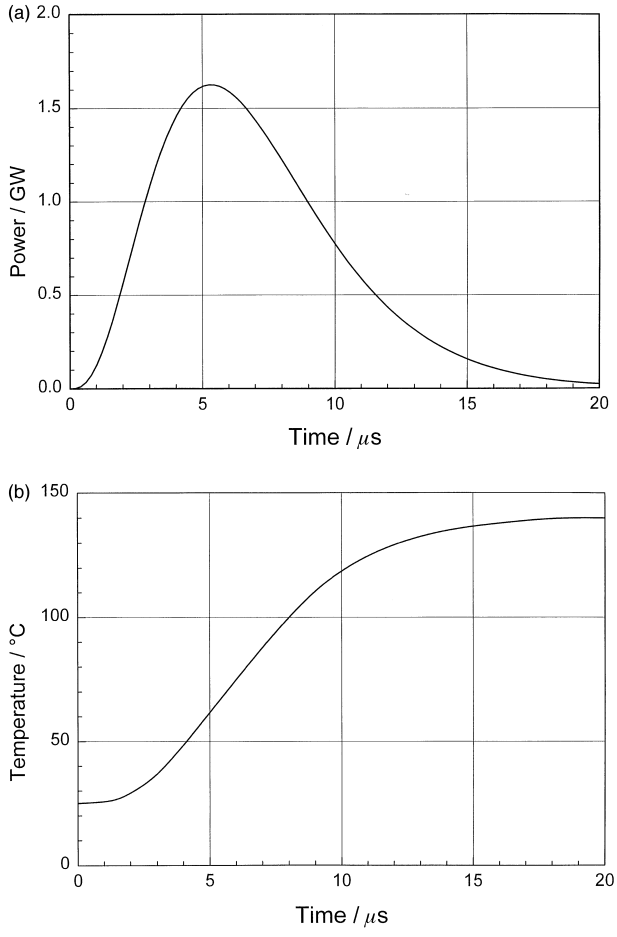

Fig. 1. (a) Applied electric power pulse and (b) the corresponding temperature raise in the varistor.

2.2. FEM-modelling

In general a varistor has a cylindrical shape and thus is axially symmetric. A free-standing varistor also possesses a midplane symmetry. Its surface is traction-free at any time. Using the advantage of the symmetry of geometry and loading, the three-dimensional problem is reduced to two dimensions and only a quarter-section of the varistor has to be modelled as shown in Fig. 2. A typical high-voltage ZnO-varistor of a diameter $D = 34$ mm and height $H = 44$ mm was chosen for the analysis. The FEM-mesh consists of $10 \times 30 = 300$ axisymmetric plane elements of equal size.

The mechanical loading to be applied on the structure is given by the time dependent temperature raise, which has been assumed to be the same in every point of the body. The temperature march specifying the loading of the varistor is shown in Fig. 1b. The material has been assumed to behave linearly elastic. Thermal and mechanical properties of a typical ZnO varistor material, used for the calculation, are given in Table 1. With these assumptions the finite element computation of the time dependent stress—strain field has been performed using commercially available FEM package ANSYS.[3] The time interval of 100 μs has been analysed in 100 equally spaced time steps.

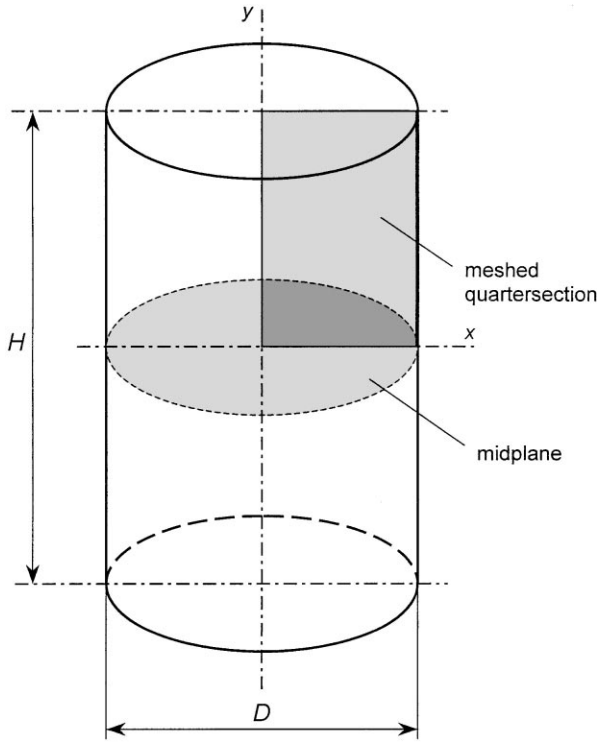

Fig. 2. Schematic representation of the FEM-model of the varistor: midplane nodes are fixed in axial direction due to the symmetry; outer surfaces are free of tractions.

Table 1
Thermal and mechanical properties of zinc oxide[5]

Elastic modulus	$E = 100$ GPa
Poisson's ratio	$\nu = 0.36$
Density	$\rho = 5420$ kg/m^3
Thermal expansion coefficient	$\alpha = 7 \times 10^{-6}$ K^{-1}
Specific heat capacity	$c_v = 550$ J/(kg K)

3. Results of the numerical stress analysis

3.1. The one-dimensional case

The axisymmetric FEM-model has been checked on the ability to simulate a 1D case and to reproduce the analytical solution of Vojta and Clarke.[1] The model describes a 1D case of a long, thin varistor if the thermal expansion coefficient and the Poisson's ratio in the radial direction are chosen to be small (e.g. 1%) compared to their actual values applied in the axial direction. The time variation of the (axial) stress in the midpoint of the varistor, as given by the model, is shown in Fig. 3, together with the analytical solution. The agreement between the numerical and analytical solutions is good. Small decay in the numerically calculated stress amplitudes is the consequence of the accumulation of computational error (numerical damping). The maximum tensile stress, which according to the 1D model occurs in the midplane, reaches about 60 MPa.

Longitudinal elastic stress waves propagate with the speed of sound, i.e. $c = \sqrt{E/\rho} = 4300$ m/s. The period of oscillation is determined by the height of the varistor, as $\tau = 2H/c = 20.5$ μs, which is correctly reproduced by the model.

3.2. The full three-dimensional analysis

An overview about designing with ceramics is given in Ref. 6. In ceramics, fracture usually originates from flaws, which act like cracks. Therefore, tensile stresses are much more dangerous than compressive stresses. Although fracture criteria for multiaxial loading conditions are still under investigation, and may depend on microstructure, the 1st principal stress is often taken to be the equivalent stress. The time history of the 1st principal stress at a selected point is shown in Fig. 4 for both the 3D and the 1D case. It can clearly be seen that the stress state in the 3D case is much more severe. Again, the mean oscillation period is about 20 μm. The maximum peak value is reached during the first oscillation period.

Critical for brittle fracture are the highest tensile stress amplitudes reached at each single point. Therefore, of relevance is the time envelope of the maximum

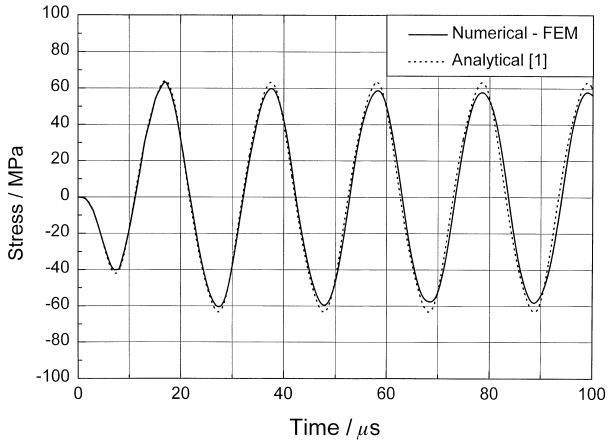

Fig. 3. Comparison of the analytically and numerically calculated axial stresses in the midpoint of the varistor in 1D case.

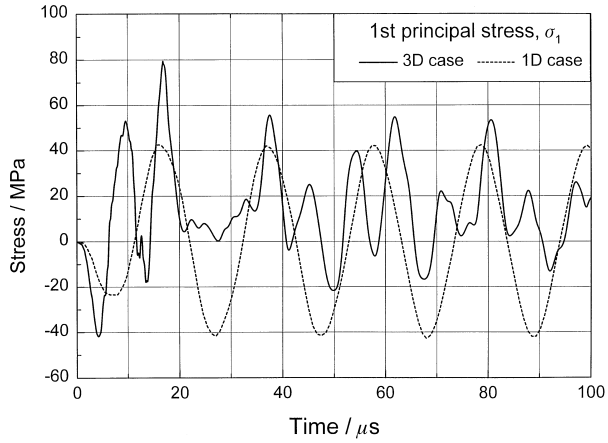

Fig. 4. History of the 1st principle stress in the volume element of highest load amplitude for the 1D and the 3D case.

first principal stress[7] which is presented in Fig. 5. The maximum load amplitude of about 80 MPa is reached on the axis of the varistor in a distance of about $H/4$ from the midplane (in fact, this is the point for which the stress history has been shown in Fig. 4). The maximum 1st principal stress in this point has axial direction. Because of the mirror symmetry there are two critical locations for failure. The maximum stresses reached are close to the typical value of mean strength of the varistor ceramics, which lies around 100 MPa. Due to an inherently wide scatter of strength of ceramics a considerable number of varistors could be expected to fail under the applied load. This is also observed during standard final quality testing.

The comparison of the results of the full 3D analysis with those obtained by applying the 1D model shows that the 1D model is not able to correctly predict neither the height nor the position of the critical stress amplitudes. Considering the typically high scatter in strength and its consequences on the probability of failure (described by the Weibull theory[8,9]) the difference

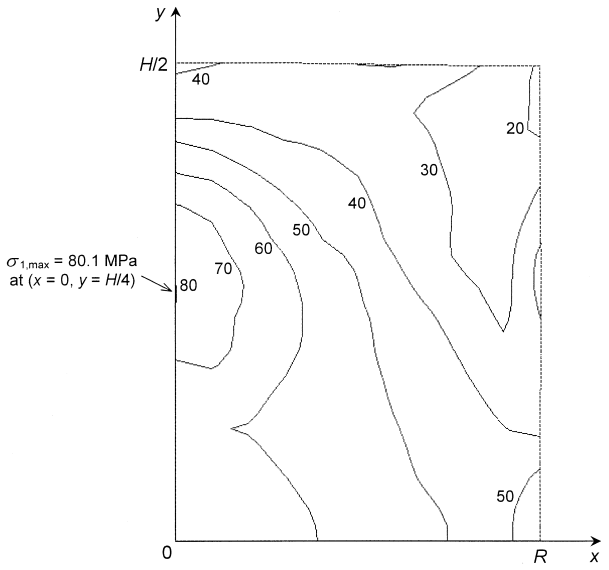

Fig. 5. Time envelope of the maximum 1st principal stress for the first 100 μs (in MPa).

between 60 and 80 MPa in the maximum applied stress amplitude leads to a significant increase of several orders of magnitude in the probability of failure (for a material with a characteristic strength of $s_0 = 100$ MPa and with a Weibull modulus of $m = 20$, the probability of failure at $\sigma = 80$ MPa is 1.2% and at $\sigma = 60$ MPa it is 3.7×10^{-3}%). Such a difference can lead to a fully erroneous prediction of the behaviour of a varistor in test conditions and an unexpectedly high waste of products.

3.3. Influence of the geometry

The position, amplitude and time of maximum stress reached is determined by the geometry as shown in Fig. 6. Accordingly, the peak stress can be minimized by choosing the optimal aspect ratio of about 0.9. The volume of the varistor should be kept constant in order to keep the thermal loading (input of Joule energy) unchanged. Compared to the varistor analyzed before, the peak stress is about 25% lower. This is also confirmed by the fracture behaviour of several types of varistors in practice.

For varistors with an aspect ratio less than about 0.5, the maximum 1st principal stress is normal to the axis. At higher aspect ratios it has axial direction. In the case of very thin varistors, the axial stresses are negligible and only the in-plane stresses are decisive for failure. In the case of a very long varistor axial stresses predominate and other stress components tend to zero. In this sense the occurrence of a minimum is connected with the transition between the regions where different stress components are predominating. The position and height of the minimum shown in the diagram in Fig. 6 depend on the details of the complex wave interference.

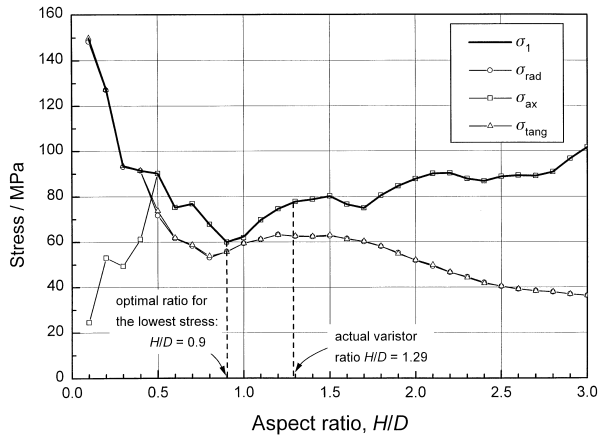

Fig. 6. Dependence of the maximum 1st principle stress on the aspect ratio of the varistor.

3.4. Influence of damping

Elastic waves lose energy due to internal friction, which is manifested as a decay in stress amplitudes. If the damping increases, the decrease of stress amplitudes is enhanced and the situation can be reached where any oscillation is suppressed and the stress monotonically decreases with time. The smallest damping that prevents oscillations is known as critical damping. In general the damping behaviour can be described by the damping ratio ξ, as the ratio of the actual to the critical damping. The influence of the damping ratio on the maximum value of the 1st principal stress reached (at the same point as in Fig. 4) is shown in Fig. 7.

To the authors knowledge measured damping values for ZnO do not exist. A rough estimate based on the sound ease off behaviour of a tolled varistor gives a damping ratio of about 10^{-3}. For this ratio the maximum 1st principle stress is reduced from 80 to 79 MPa. Only damping ratios above 10^{-2} would lead to a significant decrease of the highest 1st principle stress reached. Such high damping ratios are not likely to occur in ZnO and, therefore, the influence of damping is negligible.

3.5. Influence of the electrodes

During testing or in service a varistor is not free-standing. Its motion in axial direction is restricted to some extent by the electrodes. This influences the mechanical boundary conditions and, as a consequence, it also influences the stress state: At the boundaries between the varistor and the electrodes the elastic waves are not fully reflected as in the case of a free-standing varistor. A part of them is transferred into the electrodes. After the reflection from the back side of the electrodes a fraction of this wave can be transferred back into the varistor and will then interfere with other elastic

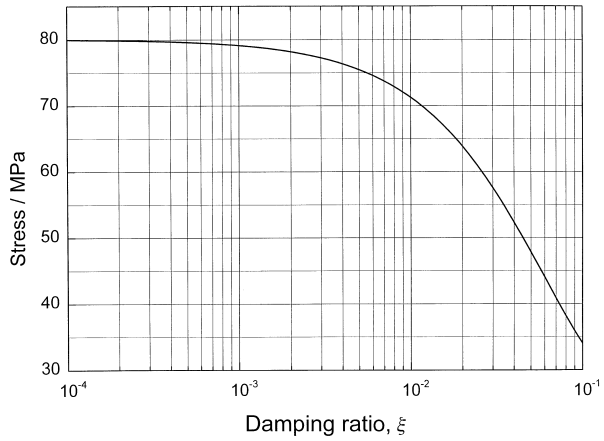

Fig. 7. Dependence of the maximum 1st principle stress on the damping ratio ξ for the same point as in Fig. 4.

waves. This complicated interference strongly depends on the geometrical details of the electrode system and also on the generally not well known details of the contact between them and the varistor. Therefore, it has been neglected in the present model. However, it can be assumed that the solution for a free-standing varistor gives an upper bound for the tensile stress amplitudes within a non-free-standing varistor. Firstly, in the free-standing case, the stress maximum always occurs within the first wave cycle. This is not likely to be different in the non-free-standing case, where the elastic strain energy in the varistor at the end of this cycle is reduced due to the energy transfer into the electrodes. Secondly, the electrodes are of a similar or higher thickness compared to that of the varistor and the wave velocity within the electrode and the varistor material is also similar. Therefore, the backscattering of energy from the electrodes into the varistor is only possible after the first wave cycle is completed. As a final consequence, the tensile stresses during the first cycle, which is most likely to be critical, will be reduced at any position. Furthermore, depending on the material and the actual geometry of the electrodes, and on the contact conditions between them and the varistor, some energy will be dispersed and dissipated in the electrode system. This will further contribute to a reduction of tensile stresses in the varistor in the first wave cycle (after the reflection) as well as in all subsequent cycles. Additionally, clamping of the varistor between the electrodes imposes static compressive stresses which are superposed to the transient stress field and further reduce the tensile stresses.

4. Conclusions

- High voltage varistors are shock loaded with severe electrical pulses, which causes significant mechanical stresses in consequence of inertial forces appearing due to rapid Joule heating accompanied by rapid thermal elongation.
- A semiquantitative analysis of these stresses can be performed using the analytical 1D model proposed by Vojta and Clarke,[1] but a full 3D stress analysis is necessary to find out the actual location and height of the maximum tensile stresses reached. The stresses in the full 3D analysis are essentially higher than those estimated applying the 1D model.
- Critical area for the onset of fracture is on the cylinder axis. Its exact position between the midplane and the base of the varistor is determined by the aspect ratio of the varistor and tends to be in the middle only for very slender cylinders. Due to the mirror symmetry, generally there are two critical areas for failure.
- The maximum tensile stresses reached can be minimized by choosing an appropriate aspect ratio. For the analyzed case of a free standing varistor under the specific electrical loading conditions the optimal height to radius ratio is found to be 0.9.

References

1. Vojta, A. and Clarke, D. R., Electrical-impulse-induced fracture of zinc oxide varistor ceramics. *J. Am. Ceram. Soc.*, 1997, **80**, 2086–2092.
2. Zienkiewicz, O. C., *The Finite Element Method in Engineering Science*, 3rd edn. McGraw-Hill, London, 1977.
3. Kohnke, P., (ed.), *ANSYS Theory Reference,* Rel. 5.3, 7th edn., ANSYS, Inc., Houston, PA, 1996.
4. Nowacki, W., *Dynamic Problems of Thermoelasticity*. Noordhoff International Publishing, Leyden, 1975.
5. Shackleford, J. F., Alexander, W. and Park, J. S., *Materials Science and Engineering Handbook*. CRC Press, Boca Raton, FL, 1994.
6. Rubeša, D., Distinctions between designing with brittle and ductile materials (submitted for publication.)
7. Fischer, F. D., Yan, W. Y. and Danzer, R., Application of probabilistic fracture mechanics to a dynamic loading situation on the example of a dynamic tension test for ceramics *J. Eur. Mat. Sci.*, in press.
8. Weibull, W., *A Statistical Theory of the Strength of Materials,* Ingeniörsvetenskapsakademiens Handligar Nr. 151, Stockholm, 1939.
9. Danzer, R., A general strength distribution function for brittle materials. *J. Eur. Ceram. Soc.*, 1992, **10**, 461–472.